Acoustoelectric Effects in Indium Antimonide*

W. J. FLEMING AND J. E. ROWE
Electron Physics Laboratory, Department of Electrical Engineering, The University of Michigan, Ann Arbor, Michigan 48104
(Received 13 August 1970)

The acoustoelectric interaction in InSb is developed and investigated on the basis of a hydrodynamical theory. Comparison of numerical results obtained from this theory with the corresponding numerical results from more detailed microscopic theories reveals that the essential features of the microscopic theories are also present in the simpler hydrodynamical theory. In particular, the hydrodynamical theory accounts for the existence of two distinct modes of acoustic domain formation and for the reduction of peak acoustic gain at low values of magnetic field. Valuable insight into the physical basis of the acoustoelectric effect is obtained and it is shown that in the limit of large electron drift velocities and small transverse magnetic field strengths, the Mode I-type acoustoelectric interaction arises from a drift-enhanced quenching of electron diffusion effects. Moreover it is found that the frequency of maximum acoustoelectric gain, as given by the hydrodynamical theory of the present paper, does not occur at the fixed frequency $f_0=(\omega_R\omega_D)^{1/2}/2\pi$, but rather, it is dependent upon the exact values of drift velocity and magnetic field strength. Several computer-generated plots are presented and discussed in order to fully illustrate the results of this investigation.

I. INTRODUCTION

Whenever the applied transverse magnetic field strength and the sample current in InSb exceed certain threshold levels, acoustic domains form in ⟨110⟩-oriented n-InSb at 77°K. Although the presence of these acoustic domains limits the utility of the acoustoelectric amplification process,[1,2] the domains are interesting in themselves. The acoustic domains are manifested by the appearance of rf current oscillations and microwave noise radiation which in turn have been the subject of numerous investigations.[3–6] It has been found experimentally that, in sufficiently long specimens of InSb, both phenomena possess nearly identical applied field threshold dependences and exhibit two distinct modes of operation. Mode I occurs for high current values and low magnetic-field strengths, whereas Mode II occurs in the opposite limits. Recently it has been concluded by several investigators that although the magnetic field enhanced hydrodynamical theory of Steele[7] and Turner *et al.*[8] can account for Mode II operation, more detailed microscopic theories[1,9,10] are required to adequately account for the existence of both Modes I and II. The results presented in this paper will show that a hydrodynamical theory, which is an extension of the theory of Steele[7] and Turner *et al.*,[8] not only accounts for both Mode I and Mode II operation but also yields valuable insight into the physical basis of the acoustoelectric effect in InSb. It is well known that the Mode II acoustoelectric interaction arises from a magnetic field enhancement of the rf magnetoresistance.[7,8] Investigation of the hydrodynamical theory of the present paper shows that the Mode I acoustoelectric interaction arises from a different physical mechanism, namely, a drift-enhanced quenching of diffusion effects.

II. HYDRODYNAMICAL THEORY OF ACOUSTOELECTRIC EFFECTS IN InSb

The derivation and notation of this theory follows that of Steele[7] and Turner *et al.*[8] and other related work[4,11]; the theory of Steele[7] and Turner *et al.*[8] will hereinafter be referred to as the STVW theory.

In the theory of microscopic interactions a detailed analysis of the conduction electron trajectories is undertaken and it is found that Doppler-shifted cyclotron resonances occur as a consequence of the finite cyclotron radius of the electrons gyrating about the applied magnetic field. However, under the operating conditions of interest,[1–6] such interaction can only occur in the presence of small magnetic fields whereupon collisions will broaden and weaken the resonance.[1] In the theory of hydrodynamical interactions, macroscopic averages or moments of the Boltzmann equation are utilized and the detailed analysis of the electron trajectories is ignored. Despite the fact that the hydrodynamical theory does not take resonance effects into account, it is nevertheless asserted that a hydrodynamical description of the rf conductivity is adequate to study acoustoelectric effects in InSb (comparison of numerical results obtained from this theory with results obtained from the more complete microscopic theories[1,9,10] has shown that this is indeed a good approximation). The drifting electron stream and attendant space-charge waves are described by the equation of momentum conservation, Maxwell's equations, and equations of charge continuity which are, respectively (neglecting trapping effects):

$$(\partial\mathbf{v}/\partial t)+(\mathbf{u}_0\cdot\nabla)\mathbf{v}=(Q/m^*)(\mathbf{E}+\mathbf{u}_0\times\mathbf{B}+\mathbf{v}\times\mathbf{B}_0)-\nu\mathbf{v}-(v_T^2/N_0)\nabla n, \quad (1)$$

$$\nabla\times\mathbf{E}=-(\partial\mathbf{B}/\partial t), \qquad \nabla\cdot\mathbf{B}=0, \quad (2)$$

and

$$\mathbf{J}=Q(N_0\mathbf{v}+n\mathbf{u}_0), \qquad \nabla\cdot\mathbf{J}+Q(\partial n/\partial t)=0, \quad (3)$$

where $\mathbf{v}$, n, $\mathbf{E}$, $\mathbf{B}$, and $\mathbf{J}$ are the first-order perturbed transport and field variables; $\mathbf{u}_0$, N_0, $\mathbf{E}_0$, $\mathbf{B}_0$, and $\mathbf{J}_0$ are the corresponding static values of the transport and field variables; and the assumed-constant phenomenological constants ν, Q, m^*, and v_T are, respectively, the momentum relaxation collision frequency, the electron

TABLE I. Physical parameters for n-type InSb at 77°K.

Parameter	Symbol	Value
Electron effective mass	m^*	$0.013\ m_0$
Sound velocity[a]	v_s	2.33×10^5 cm/sec
Carrier concentration	N_0	1×10^{14} cm^{-3}
Lattice dielectric constant	ϵ_l	$17.8\ \epsilon_0$
Thermal velocity[b]	v_T	3×10^7 cm/sec
Carrier mobility	μ	6×10^5 cm^2/V sec

[a] This value of the sound velocity is appropriate for the fast-transverse acoustic wave propagating along a ⟨110⟩-crystallographic direction in InSb.
[b] The average electron thermal velocity is determined by $v_T=(k_BT_L/m^*)^{1/2}$, where k_B is Boltzmann's constant and T_L is the average carrier temperature which is taken here as 77°K.

charge, the effective electron mass, and the average thermal velocity of the electrons.

Assuming that acoustic waves propagate in the x direction with wave vector $\mathbf{q}=(\omega/v_s)\hat{x}$, that all the perturbed transport and field quantities vary as $\exp[j(\omega t-\mathbf{q}\cdot\hat{x})]$, and that an applied magnetic field $\mathbf{B}_0=B_\perp\hat{z}$ and an applied current $\mathbf{J}_0=QN_0(u_{0x}\hat{x}+u_{0y}\hat{y})$ are present; the rf conductivity tensor, defined by $\mathbf{J}=\boldsymbol{\sigma}\cdot\mathbf{E}$, is derived from Eqs. (1)–(3). Only the σ_{xx} component of $\boldsymbol{\sigma}$ is important and this is given by

$$\sigma_{xx}=\frac{(\epsilon_l\omega_R/\nu')}{(\gamma-j\omega/\omega_D\nu')}, \tag{4}$$

where ϵ_l is the lattice dielectric constant, $\omega_R=Q^2N_0/m^*\nu\epsilon_l$ is the dielectric relaxation frequency, $\gamma=1-u_{0x}/v_s$ is the drift ratio, $\omega_D=\nu v_s^2/v_T^2$ is the diffusion frequency at synchronism, $j=(-1)^{1/2}$, $\nu'\equiv(\bar{\nu}/\nu)[1+(b\nu/\bar{\nu})^2]$, $\bar{\nu}\equiv\nu+j\omega\gamma$, and $b=QB_\perp/m^*\nu$ is the dimensionless $\mu B_\perp$ product. Since the electromechanical coupling constant κ^2 of the active fast-transverse acoustic wave is much smaller than unity in ⟨110⟩-oriented InSb and the sound velocity v_s is much smaller than the velocity of light in InSb, the acoustoelectric interaction growth rate is given quite generally by

$$\alpha_{\mathrm{Re}}=-(\kappa^2\omega/2v_s)\ \mathrm{Im}[1/(1-j\sigma_{xx}/\omega\epsilon_l)], \tag{5}$$

where the wave number q has been written as $q=\omega/v_s-j\alpha$ by assuming that $|\alpha|\ll\omega/v_s$. The growth rate appears in the acoustic wave amplitude factor as $\exp(\alpha_{\mathrm{Re}}x)$, where $\alpha_{\mathrm{Re}}=-\mathrm{Re}(\alpha)$. Defining $\nu'=\nu_{\mathrm{Re}}'+j\nu_{\mathrm{Im}}'$ and substituting (4) into (5) gives the following expression for the acoustoelectric growth rate:

$$\alpha_{\mathrm{Re}}=-\kappa^2\frac{\omega_R}{2v_s}\frac{\gamma\nu_{\mathrm{Re}}'}{[(\gamma\nu_{\mathrm{Re}}')^2+(W-\gamma\nu_{\mathrm{Im}}')^2]}, \tag{6}$$

where $\nu_{\mathrm{Re}}'=1+b'^2$, $\nu_{\mathrm{Im}}'=\omega_\nu(1-b'^2)$, $b'^2\equiv b^2/(1+\omega_\nu^2)$, $\omega_\nu\equiv\omega\gamma/\nu$, and $W\equiv\omega_R/\omega+\omega/\omega_D$. Equation (6) can be rearranged in a more meaningful form as

$$\alpha_{\mathrm{Re}}=-\kappa^2(\omega_R'/2v_s)\cdot\gamma/(\gamma^2+W'^2), \tag{7}$$

where $\omega_R'=\omega_R/\nu_{\mathrm{Re}}'$ is the effective relaxation frequency, $W'\equiv(\omega_R'/\omega)+(\omega/\omega_D')$, and $\omega_D'=\omega_D\nu_{\mathrm{Re}}'/(1-\gamma\nu_{\mathrm{Im}}'\omega_D/\omega)$ is the effective diffusion frequency.

Although Abe and Mikoshiba[12] have previously published a derivation of this type, there is an error in their σ_{xx}-conductivity expression wherein terms of the form $\omega_\nu u_{0x}/v_s$ which appear in the denominator of (2) of Ref. 12 should not be present.[13,14] The algebraic definitions for a_1 and a_2 used by Abe and Mikoshiba[12] lead to a particularly complicated expression for α_{Re} which is nonetheless identical (when corrected[13]) to the expression for α_{Re} given by (7) of the present paper.

When inertial terms are neglected, $\omega_\nu\to0$, (7) reduces to the corresponding hydrodynamical result of the STVW theory.[7,8] When the magnetic field is zero, $b\to0$, (7) reduces to the corresponding hydrodynamical result of Kino and Route[4]; and when both inertial terms and magnetic field effects are neglected, $\omega_\nu\to0$ and $b\to0$, (7) reduces to the corresponding hydrodynamical result of White.[11]

III. ANALYSIS OF THE HYDRODYNAMICAL THEORY

A fixed maximum value of the acoustoelectric interaction growth rate, equal to $\kappa^2(\omega_R\omega_D)^{1/2}/8v_s$, is given by the STVW theory and it occurs at $-\gamma(1+b^2)=W_{\min}$, where $W_{\min}=2(\omega_R/\omega_D)^{1/2}$ when $\omega=\omega_0=(\omega_R\omega_D)^{1/2}$. Using the physical parameters in Table I and normalizing the acoustoelectric interaction growth rate to κ^2; the quantity $\alpha_{\mathrm{Re}}/\kappa^2$, which is labeled "gain," has been plotted as a function of a normalized drift ratio $\Gamma\equiv(u_{0x}-v_s)/v_T=-v_s\gamma/v_T$. The results are shown in Fig. 1. In this figure and in all of the following figures, u_0 is the u_{0x}-drift component and normalized gain is plotted in

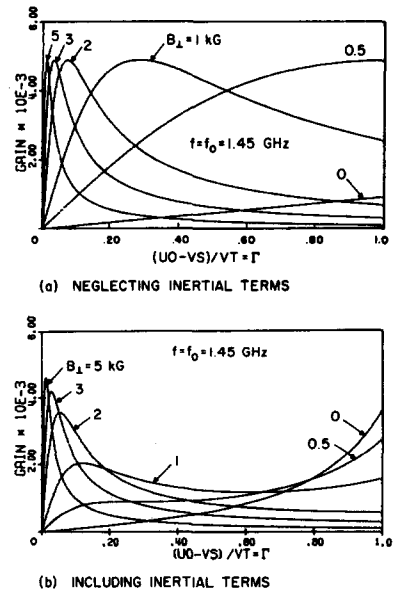

FIG. 1. Acoustic gain $\alpha_{\mathrm{Re}}/\kappa^2$ as a function of drift velocity u_0.

units of rad/cm. In Fig. 1(a) the results for the STVW theory are shown and in Fig. 1(b) the results for the present theory, using (7), are shown. If no magnetic field is present, the value $\Gamma=1$ gives $J_0=484$ A/cm^2 and $E_0=50.3$ V/cm. It is seen in Fig. 1(b) that when inertial terms are included, the maximum value of the acoustoelectric interaction growth rate becomes strongly dependent on the strength of the applied magnetic field. Comparison of Fig. 1(b) with the numerical results of corresponding microscopic theories[1,10] shows that no essential difference exists between the results of the hydrodynamic theory of the present paper and the more complete microscopic theories.[1,10]

In Fig. 2, gain is plotted as a function of magnetic field strength for selected values of the drift ratio Γ. Harth and Jaenicke[9] have plotted the corresponding results for the microscopic theory. Aside from the

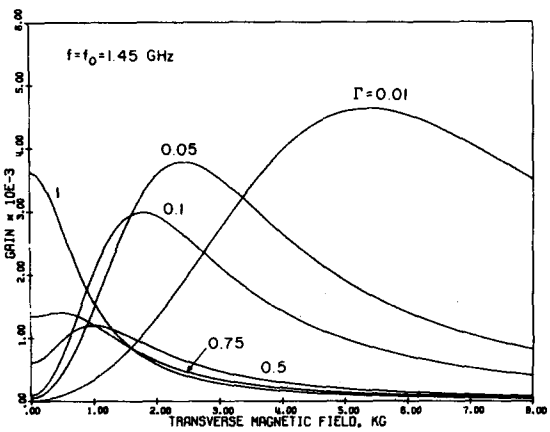

FIG. 2. Acoustic gain α_{Re}/κ^2 as a function of transverse magnetic field $B_\perp$.

appearance of some relatively subdued cyclotron resonance effects, the present theory and the microscopic theory[9] give nearly identical results (for reasonable drift velocities, i.e., $u_0 \lesssim 0.5 v_T$).

The relative simplicity of (7) has permitted a detailed investigation of its behavior. Using the numerical methods of interval halving and false position, level curves have been computer generated and one set, obtained at the frequency $f_0=(\omega_R\omega_D)^{1/2}/2\pi$ is shown in Fig. 3. The emergence of Mode I operation[3,6] in the region of low magnetic field strengths and high drift velocities is apparent. The general structure of the level curve set in Fig. 3 is very similar to the corresponding results from microscopic theory (Fig. 2 of Ref. 9). The maximum and minimum values of acoustic gain at $f=f_0$ are found from searching the region bounded by $0\leqq B_\perp\leqq 5$ kG and $0\leqq\Gamma\leqq 1$ and are plotted in Fig. 4. A transition region whereupon Mode I and Mode II exist concomitantly,[6] depending on the value of the drift ratio, is evident in the neighborhood of $B_\perp=1$ kG. In

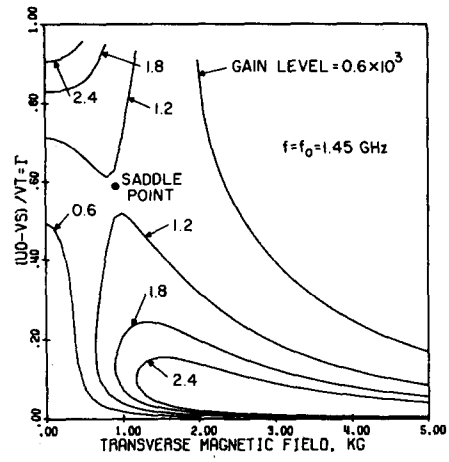

FIG. 3. Gain level curves at 1.45 GHz.

Fig. 4, the following extrema branches are identified:

(1) Branch I, $0\leqq B_\perp\lesssim 1.9$ kG, is a line of absolute maxima which occurs along $\Gamma=1$ and corresponds to maximum Mode I gain.

(2) Branch II, $0.5\lesssim B_\perp\leqq 5$ kG, is a line of relative maxima Mode II gain and approaches the STVW theoretical maximum gain at large values of magnetic field.

(3) Branch III, $0.5\lesssim B_\perp\lesssim 1.9$ kG, is a line of relative minima which includes the saddle point shown in Fig. 3. The saddle point occurs at $B_\perp=0.9$ kG, $\Gamma=0.57$ with gain equal to 1.19×10^3.

(4) Branch IV, $1.9\lesssim B_\perp\leqq 5$ kG, is a line of absolute minima which occurs along $\Gamma=1$.

On Branch II in Fig. 4, a maximum gain of 4.61×10^3 is attained at $B_\perp=5$ kG, $\Gamma=0.0109$. This gain value is equal to 94.5% of the STVW theoretical maximum gain and, with $B_\perp=5$ kG, it exists at a somewhat lower drift ratio than is predicted by the STVW theory which is also equal to 94.5% of the drift ratio predicted by the STVW theory. The value of maximum gain on Branch II has diminished to 50% of the STVW theoretical maximum gain at $B_\perp=1.2$ kG, $\Gamma=0.100$. For Branch I, a maximum gain of 3.63×10^3 occurs at $B_\perp=0$, $\Gamma=1$.

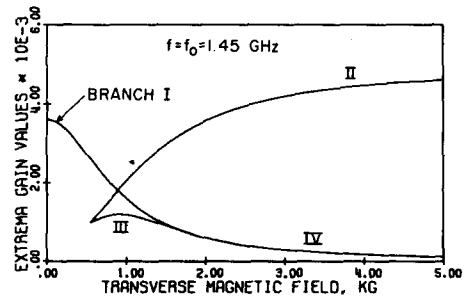

FIG. 4. Maximum and minimum gain values at 1.45 GHz.

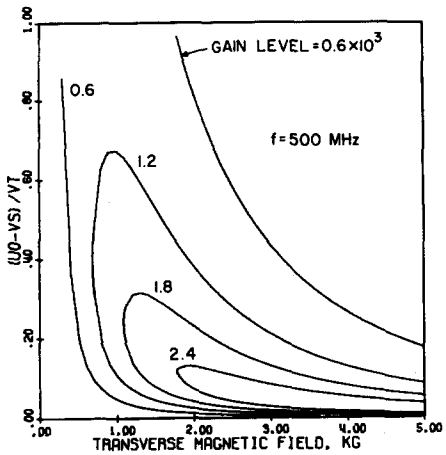

FIG. 5. Gain level curves at 500 MHz.

For comparison, a level curve set has also been computed at the frequency of 500 MHz (arbitrary) and it is shown in Fig. 5. At this frequency, all evidence of Mode I operation has disappeared[6] and deviations from the STVW theory are less significant. Using the same method as before, the extrema gain values for $f=500$ MHz are plotted in Fig. 6. Now only three extrema gain branches exist, namely, Branches I, II, and IV. On Branch II, which corresponds to the STVW theory, a maximum gain of 2.92×10^3 is attained at $B_\perp=5$ kG and $\Gamma=0.0181$; whereas the STVW theoretical maximum gain here is 3.02×10^3, occurring at $\Gamma=0.0187$. The value of maximum gain on Branch II has diminished to 50% of the STVW maximum value at $B_\perp=0.9$ kG, $\Gamma=0.293$. Branch II continues on to join with Branches I and IV at $B_\perp=0.55$ kG, $\Gamma=1$.

Finally, for completeness, a level curve set which is computed at the frequency of 10 GHz is shown in Fig. 7. At this frequency the overall gain level is approximately an order-of-magnitude smaller than it is at the lower frequencies shown in Figs. 3 and 5. Moreover, cyclotron resonance effects will be especially important in the region of Mode I operation and cannot be ignored at this high a frequency. Thus the results of the present paper diverge noticeably from the results of the microscopic theories[9,10] in the region of Mode I operation, but in the region of Mode II operation, the present theory retains validity.

An expanded view of the extrema gain values for $f=10$ GHz is shown in Fig. 8 and it is seen that only Branches I, II, and III exist. On Branch II, which corresponds to the STVW theory, a maximum gain of 1.02×10^3 is attained at $B_\perp=10$ kG, $\Gamma=0.0075$; whereas the STVW theoretical maximum gain here is 1.39×10^3, occurring at $\Gamma=0.0102$. The value of the maximum gain on Branch II has decreased to 50% of the STVW maximum value at $B_\perp=6.1$ kG, $\Gamma=0.0138$. Branches II and III join at $B_\perp\simeq0.5$ kG, $\Gamma\simeq0.050$. The saddle point, shown in Fig. 7, is located on Branch III at $B_\perp\simeq4.2$ kG, $\Gamma\simeq0.410$. On Branch I, which occurs identically along $\Gamma=1$, the gain achieves a maximum value of 64.9×10^3 at $B_\perp=0$. As discussed in Sec. IV, the maximum achievable Mode I gain is given by $\omega_R/2v_T$ which equals 101.8×10^3 for the parameters used here. Thus at the frequency of 10 GHz, which equals $6.9f_0$, it is found that 64% of the maximum achievable Mode I gain has been attained.

IV. PHYSICAL MECHANISM OF MODE I OPERATION

The uncomplicated hydrodynamical derivation of the present theory permits an investigation of the fundamental physical mechanism which gives rise to Mode I operation.

Kino and Route[4] first examined the zero-magnetic-field hydrodynamic theory and they showed that the maximum acoustoelectric interaction growth rate occurs for $b=0$ and $\omega_\nu\neq0$, at the frequency

$$\omega_0'=(\omega_R\omega_D)^{1/2}/(1-\Gamma^2)^{1/2}, \tag{8}$$

where $\Gamma=(u_{0x}-v_s)/v_T=-v_s\gamma/v_T$. They also pointed out that in order to achieve the maximum growth rate, the drift velocity must approach the value of the thermal velocity which, by (8), indicates that maximum growth rates can only be achieved at extremely high frequencies. They did not pursue this point further, concluding that at these high frequencies the hydrodynamic theory is no longer applicable.[4] However, as the numerical results of Sec. III have shown, the hydrodynamic theory of the present paper nevertheless exhibits the same Mode I operation as is exhibited by the corresponding microscopic theories.[1,9,10] It has been previously concluded[9,10] that Mode I operation must arise from effects such as cyclotron resonance which are only described by the complete microscopic theory. It will now be shown that the hydrodynamic theory of Sec. II accounts for Mode I operation through a diffusion quenching mechanism.

As discussed in Sec. III, numerical calculations show that maximum Mode I gain is found for zero magnetic field. Taking $b=0$, the maximum Mode I gain is determined from (7) by setting $d(\alpha_{\mathrm{Re}})/d\gamma=0$, and it is found

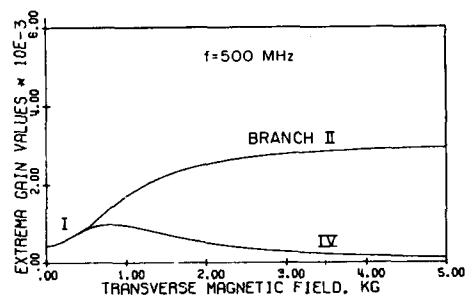

FIG. 6. Maximum and minimum gain values at 500 MHz.

that the maximum gain is

$$(\alpha_{\mathrm{Re}})_{\max}=\kappa^2\omega_R/2v_T \tag{9}$$

occurring at

$$\gamma^2=(v_T^2/v_s^2)\,(1+\omega_R\omega_D/\omega^2), \tag{10}$$

where the inequality $2\omega W\gg\nu$, which is satisfied for all values of ω, has been employed. This value of maximum gain, (9), is equal to $4(\omega_R/\nu)^{1/2}$ times the STVW theoretical maximum gain and, more significantly, corresponds to the maximum attainable gain of White's theory[11] in the limit $\omega_D\to\infty$, $\gamma=-v_T/v_s$. Although the maximum gain given by (9) can only be obtained for a drift velocity approximately equal to the thermal velocity, this maximum gain is $4(\omega_R/\nu)^{1/2}$ times greater than that of the STVW theory and this ratio ranges from 10 to 20, depending on the value of transport parameters ω_R and ν. The numerical results of Sec. III have shown that merely approaching the condition of maximum gain while maintaining reasonable drift velocities, $u_0\lesssim 0.8v_T$, will give Mode I gain values comparable to the STVW maximum Mode II gain value. Additional studies[14] of the acoustoelectric interaction growth rate, wherein an empirical field-dependent mobility saturation effect is incorporated into (7), shows that for intermediate drift ratios $0.2\lesssim\Gamma\lesssim 0.9$, the Mode I gain mechanism is further enhanced by a factor of up to 2.5 when mobility saturation effects are included. It is found[14] that the onset of Mode I operation at $f=f_0$ appears at drift ratios as low as 0.4 where the present hydrodynamical theory retains validity.

The physical mechanism of Mode I operation in terms of the present hydrodynamical theory can now be readily understood. In the acoustoelectric interaction, it can be shown[15] that diffusion effects are characterized by a diffusion time τ_D which is approximately equal to ω_D/ω^2. When inertial terms are included and no magnetic field is present, the effective diffusion frequency ω_D becomes, from (7), $\omega_D'=\omega_D/(1-\Gamma^2)$. As $u_{0x}\to v_T$ and $\Gamma\to 1$, the effective diffusion frequency ω_D' approaches

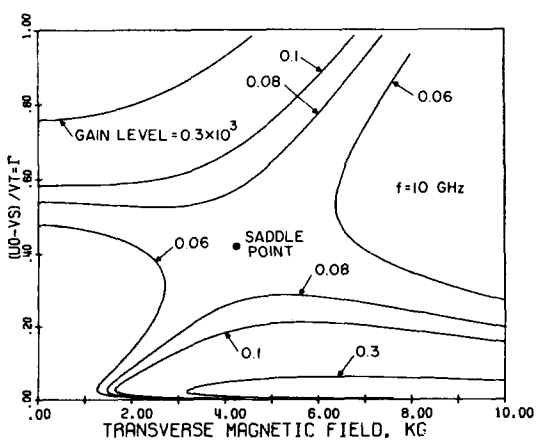

FIG. 7. Gain level curves at 10 GHz.

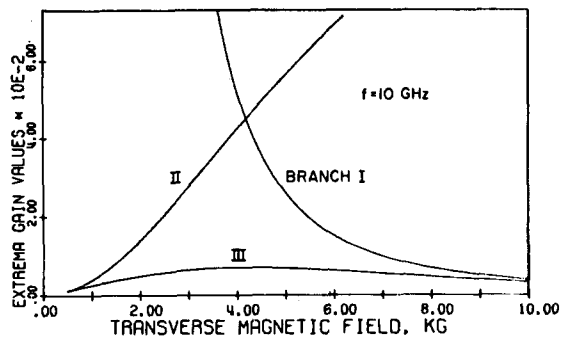

FIG. 8. Maximum and minimum gain values at 10 GHz.

infinity. At a given frequency, this gives an infinitely long diffusion time τ_D which allows for more effective space-charge bunching of the streaming electrons. In fact, some preliminary algebra combining (1) and (3) shows that the condition $\Gamma^2=1$, which for the purpose of exposition is rewritten as $j\omega\gamma v_x=j(v_T^2q^2/\omega\gamma)v_x$, corresponds to exact cancellation of the diffusion term by the inertial term in the equation of momentum conservation. The essential point here is that the fundamental physical mechanism of Mode I operation, as depicted by the hydrodynamical model,[16] is the quenching of diffusion effects by the drift-enhanced inertial effects of the streaming electrons, thereby allowing for more effective bunching of the electrons which results in the emergence of the Mode I operation.

From (10) it is seen that for $\omega\ll(\omega_R\omega_D)^{1/2}$, the drift velocity must be unrealistically large in order to quench diffusion effects. Thus, Mode I operation will disappear at lower frequencies as has been observed experimentally.[6]

The effect of the magnetic field on the Mode I gain mechanism is best understood by consideration of the effective diffusion frequency ω_D', defined by (7), which can be written as

$$\omega_D'=\omega_D(1+b'^2)/[1+\Gamma^2(b'^2-1)], \tag{11}$$

where $b'\equiv b/(1+\omega_\nu^2)^{1/2}$, $\Gamma=(u_{0x}-v_s)/v_T$, and $\omega_\nu=\omega\gamma/\nu$. In the limit of small drift velocities which corresponds to Mode II operation, ω_ν and Γ approach zero thereby reducing (11) to $\omega_D'=\omega_D(1+b^2)$ in accordance with the STVW theory. However for Mode I operation, ω_ν and Γ can no longer be ignored. As pointed out above, when $b=0$ and $\Gamma\to 1$, $\omega_D'\to\infty$. Examination of (11) in the limit $\Gamma=1$ shows that, as the magnetic field is increased from zero to a value such that $b'^2\gg 1$, the effective diffusion frequency decreases monotonically from $\omega_D'=\infty$ to $\omega_D'=\omega_D$. This means that the diffusion quenching effects which are present when $b\simeq 0$ have been eliminated by the presence of a sufficiently large magnetic field. The disappearance of Mode I operation with increased magnetic field strength is observed experimentally[3,4,6] to occur in the neighborhood of 1 to 2 kG. Taking

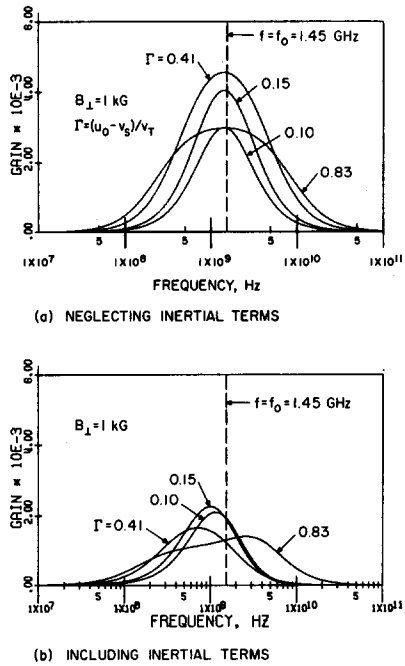

FIG. 9. Frequency dependence of the acoustoelectric gain.

$\omega=(\omega_R\omega_D)^{1/2}$, $\Gamma=1$, and using the parameters in Table I, the condition $b'^2=1$ occurs at $B_\perp\simeq 0.9$ kG. As seen in Figs. 2 and 3, at $B_\perp\simeq 0.9$ kG the Mode I gain has been reduced to less than one half its zero-magnetic-field value.

Physically, examination of Eqs. (1)–(3) shows that the presence of a magnetic field together with large drift velocities, gives rise to a coupling of the transverse v_y component of the space-charge wave to the longitudinal v_x component. The strong coupling effects enter via the rf Lorentz force term in (1). When $\Gamma^2>\frac{1}{2}$ and $b'^2\gg 1$, (11) shows that diffusion quenching effects are eliminated and the Mode I gain mechanism is diminished. However for $\Gamma^2<\frac{1}{2}$, the effective diffusion frequency given by (11) is enhanced by the presence of a magnetic field and the STVW Mode II gain mechanism emerges.

V. FREQUENCY DEPENDENCE OF THE ACOUSTOELECTRIC GAIN

Further analysis reveals that unlike the STVW theory, the acoustoelectric gain expression of the present theory, (7), is not logsymmetric about the frequency $f_0=(\omega_R\omega_D)^{1/2}/2\pi$. The frequency dependence of the acoustoelectric gain for the STVW theory is shown in Fig. 9(a) and the corresponding results for the present theory are shown in Fig. 9(b). It is seen in Fig. 9(b) that for low drift velocities with $\Gamma\lesssim 0.75$, the frequency of maximum gain is less than f_0 whereas for larger drift velocities with $\Gamma\gtrsim 0.75$, the frequency of maximum gain occurs at frequencies greater than f_0. Numerically, it has been found that the maximum achievable gain for $B_\perp=1$ kG and $\Gamma<0.75$ is equal to 2.26×10^3 and it occurs at $f=1.02$ GHz with $\Gamma=0.15$ as shown in Fig. 9(b). For $B_\perp=1$ kG, the STVW theory gives a maximum gain of 4.89×10^3 at $f=f_0=1.45$ GHz with $\Gamma=0.28$.

Although the acoustoelectric gain expression of the present theory which is given by (7) appears relatively simple, substitution of all the defined quantities shows that, as an explicit function of frequency, it is given by a ratio of a sixth-degree polynomial to an eighth-degree polynomial in terms of frequency. Because of this complexity it has been analyzed numerically, using the method of interval halving, in order to solve for the frequency of maximum gain. Taking fixed values of magnetic field and drift velocity, (7) is numerically searched for the frequency at which maximum gain is achieved and the resulting solutions, normalized to the frequency f_0, have been plotted in Fig. 10(a). In Fig. 10(b) a parameter called normalized gain is plotted; the normalized gain is defined as the ratio of the resulting maximum gain which is achieved by operating at the frequency of maximum gain, divided by the gain which exists at the fixed frequency f_0.

Figure 10(a) shows that with a sufficiently large magnetic field present, the frequency of maximum gain first occurs below f_0. Then, as the drift velocity approaches the thermal velocity ($\Gamma\to 1$), the frequency of maximum gain returns to f_0 and finally approaches infinity at $\Gamma=1$. Examination of (7) in the limit $\omega_\nu^2\gg b^2>1$, explains why the frequency of maximum gain approaches infinity at $\Gamma=1$. In the aforementioned

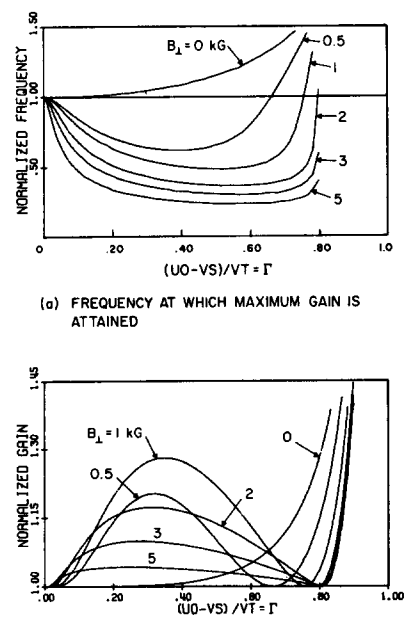

FIG. 10. Maximum acoustoelectric gain.

limit, (7) again reduces to the hydrodynamical theory of Kino and Route[4] (it was first shown to reduce to this theory when $b=0$) and the frequency of maximum gain is given by (8). As (8) shows, when $\Gamma\rightarrow 1$ the frequency of maximum gain approaches infinity.

In Fig. 10(b) the normalized gain can also be considered as the fractional increase in gain which is achievable by changing operation from the frequency $f=f_0$ to the frequency of maximum gain shown in Fig. 10(a). For moderate values of the drift ratio Γ, the gain improvement is most pronounced for magnetic-field values around 1 kG whereupon the parameters ω_ν and b of (7) are comparable. For example, a 28.2% gain improvement can be achieved for $B_\perp=1$ kG at $\Gamma=0.35$ by operation at the reduced frequency of $0.525f_0=760$ MHz. When large magnetic fields exist, all the solutions for the frequency of maximum gain, shown in Fig. 10(a), cross over $f=f_0$ near $\Gamma\simeq 0.81$. At the cross-over point the normalized gain must pass through unity since the frequency of maximum gain equals f_0 at this point. Another important observation is that although the frequency of maximum gain is most markedly reduced for large values of magnetic field, the gain improvement realized by operation at this reduced frequency is marginal. For example, the minimum frequency of maximum gain shown in Fig. 10(a) is equal to $0.242f_0=$ 350 MHz and it occurs for $B_\perp=5$ kG with $\Gamma=0.60$, however only a 2.4% gain improvement is realized here. This behavior occurs because, for large values of magnetic field such that $(1+b^2)\gg W/\gamma$ [see (7)], the frequency dependence of the gain becomes broad band and the gain is fairly constant over nearly a decade of frequency variation.

Consideration of the frequency dependence of the acoustoelectric gain gives further insight into the physical mechanism of Mode I operation. Single-frequency gain results, as presented in Sec. III, are not necessarily a good indication of the strength of the acoustic domain formation process. Assuming that the acoustic domains are nucleated by the amplification of acoustic thermal flux, the domain formation results from the integrated influence on the conduction current of the broad-band thermal phonon spectrum. Only those phonons with frequencies near the frequency of maximum acoustic gain will be sufficiently amplified to contribute to the acoustoelectric field. Thus, broad-band acoustic gain is required for strong domain formation. This can occur in either of two ways. First, corresponding to the STVW theory, a large value of magnetic field is required [such that, $(1+b^2)\gg W/\gamma$] and broad-band acoustic gain will exist which leads to the emergence of Mode II domain formation. Second, as evidenced in Fig. 10, at large values of electron-drift velocity there is pronounced gain enhancement at high frequencies which dramatically broadens the acoustic gain spectrum and leads to the emergence of Mode I domain formation. Figure 10(a) shows a concise delineation between Mode I and Mode II operation. Whenever the normalized frequency of maximum gain is less than unity in Fig. 10(a), Mode II effects dominate; and when it exceeds unity, Mode I effects dominate.

* This work was supported by the Air Force Systems Command's Rome Air Development Center.

[1] R. K. Route and G. S. Kino, IBM J. Res. Develop. **13**, 507 (1969).
[2] J. Livingstone and W. Duncan, Brit. J. Appl. Phys. **2**, 1411 (1969).
[3] C. W. Turner and J. Crow, Appl. Phys. Lett. **11**, 187 (1967).
[4] G. S. Kino and R. Route, Appl. Phys. Lett. **11**, 312 (1967).
[5] C. W. Turner, J. Appl. Phys. **39**, 4246 (1968).
[6] T. Arizumi, T. Aoki, and K. Hayakawa, J. Phys. Soc. Japan **25**, 1361 (1968).
[7] M. C. Steele, RCA Rev. **28**, 58 (1967).
[8] C. W. Turner, T. Van Duzer, and K. Weller, Electron. Lett. **3**, 162 (1967).
[9] W. Harth and R. Jaenicke, Appl. Phys. Lett. **14**, 27 (1969).
[10] K. P. Weller and T. Van Duzer, J. Appl. Phys. **40**, 4278 (1969).
[11] D. L. White, J. Appl. Phys. **33**, 2547 (1962).
[12] Y. Abe and N. Mikoshiba, Appl. Phys. Lett. **13**, 241 (1968).
[13] Correcting this error, the term $\eta(\gamma-1)$ must be dropped from the definition of ξ in (9) of Ref. 12, where η equals ω_ν of the present paper and (8) of Ref. 12 remains as written.
[14] W. J. Fleming and J. E. Rowe, Appl. Phys. Lett. **18**, 96 (1971).
[15] M. C. Steele and B. Vural, *Wave Interactions in Solid-State Plasmas* (McGraw-Hill, New York, 1969), p. 143.
[16] Recent work by E. Voges (Int. Conf. Microwave Opt. Generation and Amplification, 8th Amsterdam, 1970) has shown that the fundamental physical mechanism of Mode I operation, as depicted by microscopic theory, is anti-Landau damping. Although the diffusion quenching effect of the present hydrodynamical theory and the anti-Landau damping mechanism of the microscopic theory appear to be unrelated, it is believed that for the physical parameter values for which Mode I operation occurs, quantum analysis, classical microscopic analysis, and the present hydrodynamical analysis will all yield similar results.